Food and Chemical Toxicology 133 (2019) 110764

Contents lists available at ScienceDirect

Food and Chemical Toxicology

journal homepage: www.elsevier.com/locate/foodchemtox

Metabolite profiling, arginase inhibition and vasorelaxant activity of *Cornus mas*, *Sorbus aucuparia* and *Viburnum opulus* fruit extracts

Alexandra Bujor[a,b], Anca Miron[a], Simon Vlad Luca[a,c,*], Krystyna Skalicka-Wozniak[d], Mihaela Silion[e], Robert Ancuceanu[f], Mihaela Dinu[f], Corine Girard[b], Céline Demougeot[b,**], Perle Totoson[b]

[a] Department of Pharmacognosy, Grigore T. Popa University of Medicine and Pharmacy Iasi, 16 Universitatii Street, 700115, Iasi, Romania
[b] PEPITE EA 4267, FHU INCREASE, University Bourgogne Franche-Comté, 19 Rue Ambroise Paré, F-25030, Besançon, France
[c] Biothermodynamics, TUM School of Life and Food Sciences Weihenstephan, Technical University of Munich, Maximus-von-Imhof-Forum 2, 85354, Freising, Germany
[d] Department of Pharmacognosy with Medicinal Plant Unit, Medical University of Lublin, Chodzki 1, 20-093, Lublin, Poland
[e] Institute of Macromolecular Chemistry Petru Poni, 41A Grigore Ghica Voda Alley, 700487, Iasi, Romania
[f] Department of Pharmaceutical Botany and Cell Biology, Carol Davila University of Medicine and Pharmacy, 6 Traian Vuia Street, 020956, Bucharest, Romania

ARTICLE INFO

Keywords:
Viburnum opulus
Sorbus aucuparia
Cornus mas
Arginase inhibition
Endothelium-dependent vasorelaxation
Chlorogenic acid

ABSTRACT

The present study investigated the effects of *Cornus mas, Sorbus aucuparia* and *Viburnum opulus* fruit extracts on arginase activity and arterial vasodilation. *V. opulus* fruit extract exerted the highest vasorelaxant activity in phenylephrine precontracted rat aortic rings (EC_{50} = 6.31 ± 1.61 μg/mL) and a significant inhibition of arginase (IC_{50} = 71.02 ± 3.06 μg/mL). By contrast, *S. aucuparia* and *C. mas* fruit extracts showed no important anti-arginase activity and a significantly weaker activity in the rat aortic rings relaxation assay (EC_{50} = 100.9 ± 11.63 and 78.52 ± 8.59 μg/mL, respectively). For all extracts, the main mechanism of vasodilation was proven to be endothelium-dependent. HPLC-ESI-Q-TOF-MS/MS studies revealed a very complex metabolite profiling in all three extracts with chlorogenic acid accounting for 30.89, 0.72 and 2.03 mg/g in *V. opulus*, *C. mas* and *S. aucuparia* fruit extracts, respectively. All extracts were declared non-toxic in the brine shrimp acute toxicity test. Our study highlights potential benefits of *V. opulus* fruit extract in diseases associated with endothelial dysfunction and impaired vasodilation.

1. Introduction

Cardiovascular diseases are one of the most important public health concerns being responsible for high mortality and morbidity worldwide. Annually, in the European countries, more than 3.8 million deaths are reported due to cardiovascular diseases, ischemic heart disease accounting for 20%. High blood pressure is also a major risk factor for cardiovascular events with a prevalence varying from 15.2% to 31.7% in the European population (Timmis et al., 2018). Most of the cardiovascular diseases are associated with endothelial dysfunction which predisposes to the development of atherosclerosis, thereby increasing the cardiovascular risk (Lerman et al., 2005).

Endothelial cells build an active layer which is responsible for vascular homeostasis through the synthesis and release of vasodilating (nitric oxide (NO), endothelium-derived hyperpolarizing factor, prostacyclin) and vasoconstricting (endothelin-1, thromboxane) mediators (Almeida Rezende et al., 2016). NO is a signaling molecule and a major pharmacological target in cardiovascular diseases. It is well-known that NO, generated by endothelial NO synthase (eNOS) from L-arginine, diffuses into the vascular smooth muscle cells promoting vasodilation through guanylate cyclase pathway (Hurlimann et al., 2002). Low vascular NO availability (decreased eNOS activity secondary to a

Abbreviations: Ach, acetylcholine; AUC, area under the curve; CM, *Cornus mas*; EC_{50}, concentration giving half-maximal relaxation; E_{max}, maximal relaxation percentage; eNOS, endothelial nitric oxide synthase; HPLC-DAD-ESI-Q-TOF-MS/MS, high-performance liquid chromatography with diode array detection coupled to electrospray ionization quadrupole time-of-flight tandem mass spectrometry; IC_{50}, concentration giving half-maximal inhibition; LC_{50}, median lethal concentration; LD_{50}, median lethal dose; L-NAME, N(ω)-nitro-L-arginine-methyl-ester; NO, nitric oxide; nor-NOHA, Nω-hydroxy-nor-arginine; PE, phenylephrine; SA, *Sorbus aucuparia*; VO, *Viburnum opulus*

* Corresponding author. Department of Pharmacognosy, Grigore T. Popa University of Medicine and Pharmacy, 16 Universitatii Street, 700115, Iasi, Romania.
** Corresponding author. PEPITE EA 4267, Faculty of Health Sciences, University of Franche-Comté, 19 Rue Ambroise Paré, F-25030, Besançon, France.
E-mail addresses: simon-vlad.v.luca@d.umfiasi.ro (S.V. Luca), cdemouge@univ-fcomte.fr (C. Demougeot).

https://doi.org/10.1016/j.fct.2019.110764
Received 31 May 2019; Received in revised form 8 August 2019; Accepted 15 August 2019
Available online 19 August 2019
0278-6915/

deficiency in enzyme substrate or co-factor, or high superoxide anion production) is the seminal mechanism involved in endothelial dysfunction (Le Brocq et al., 2008). Recent findings identified arginase as an important contributor to the endothelial dysfunction. Indeed, both arginase isoforms (I and II) are found in the endothelial cells where they catalyze the hydrolysis of L-arginine into urea and ornithine (Girard-Thernier et al., 2015; Minozzo et al., 2018). There is ample evidence demonstrating that an increased vascular arginase activity causes a depletion of L-arginine and consequently a reduction in NO production *via* eNOS leading to endothelial dysfunction associated with various diseases (Lucas et al., 2014). Moreover, overactive arginase also leads to an excessive production of L-ornithine, the precursor of polyamines (responsible for vascular smooth muscle cells hyperplasia) and L-proline (involved in collagen production, fibrosis and vessel stiffness) (Caldwell et al., 2015; Durante et al., 2013). Previous studies conducted in animals and humans showed that arginase inhibitors enhanced NO bioavailability thereby restoring normal vascular function (Minozzo et al., 2018; Prati et al., 2012). Natural products proved to be an important source of arginase inhibitors (Girard-Thernier et al., 2015). Among them, various polyphenols showed promising arginase inhibitory activity (Bordage et al., 2017; Girard-Thernier et al., 2015; Manjolin et al., 2013; Minozzo et al., 2018).

Cornus mas L. (Cornaceae, Cornelian cherry), *Sorbus aucuparia* L. (Rosaceae, rowanberries) and *Viburnum opulus* L. (Adoxaceae, European cranberrybush, guilder rose) are medicinal plants with well-known dietary value. *C. mas* grows in Europe, Asia and China being traditionally used in asthma, bronchitis, chronic inflammation, diabetes and liver diseases (Yigit, 2018). *S. aucuparia* is largely distributed in the Northern hemisphere and it is traditionally used for its anti-inflammatory properties (Olszewska and Michel, 2009). *V. opulus* is spread around Europe and Siberia, its fruits being often consumed as juice or jam (Kraujalytė et al., 2013). In the traditional medicine, *V. opulus* fruits have been used to treat pulmonary, stomach and kidney diseases but also high blood pressure and heart diseases (Kraujalytė et al., 2013; Velioglu et al., 2006). The fruits of all three species are important sources of polyphenols (particularly flavonoids and anthocyanins), vitamins, iridoids and organic acids (Cesoniene et al., 2012; Dinda et al., 2016; Kucharska et al., 2015; Zymone et al., 2018). However, some previously described pharmacological effects for *S. aucuparia, C. mas* and *V. opulus* fruits such as diuretic, anti-atherosclerotic and anti-spasmodic effects, respectively (Asgary et al., 2010; Olszewska and Michel, 2009) support possible cardiovascular benefits. To the best of our knowledge, there are no studies on the vasorelaxant and arginase inhibitory activities of the fruit extracts of these three species. With respect to toxicity, only *C. mas* acute oral toxicity has been evaluated (Dinda et al., 2016).

The aim of the present work was to investigate the vascular properties of *C. mas, S. aucuparia* and *V. opulus* fruit extracts, with special emphasis on their effects on arginase activity and endothelial function. The potential toxicity of the fruit extracts was evaluated using the brine shrimp toxicity test. In addition, a mass spectrometry-based metabolite profiling of the fruit extracts was performed.

2. Material and methods

2.1. Chemicals

Citric, malic, tartaric, quinic, chlorogenic and neochlorogenic acids, rutin, quercetin, catechin, epicatechin, phenylephrine (PE), acetylcholine (Ach), N(ω)-nitro-L-arginine-methyl-ester (L-NAME), Nω-hydroxy-nor-arginine (nor-NOHA), acetone, acetic acid and diethyl ether were purchased from Sigma-Aldrich (Steinheim, Germany). Liquid chromatographic grade formic acid, acetonitrile and water were acquired from J. T. Baker (Deventer, the Netherlands). All reagents used in the arginase inhibition assay were from Sigma-Aldrich (Saint-Quentin Fallavier, France), with the exception of purified bovine liver arginase I which was obtained from MP Biomedicals (Illkirch-Graffenstaden, France). The cysts of *Artemia franciscana* (Kellogg 1906) (brine shrimp) were commercially obtained from S. K. Trading (Thailand), with the origin stated as 100% from the Great Salt Lake (U.S.A.). The blend of salts used to prepare artificial seawater was obtained from Grotech GmbH (Baden-Wurttemberg, Germany). All chemicals used were of analytical grade. Pure water was obtained using an ELGA purification system (ELGA LabWater, United Kingdom).

2.2. Plant material and extraction procedure

C. mas fruits were collected in Iasi county (Romania) in October 2017. *S. aucuparia* and *V. opulus* fruits were collected in Suceava county (Romania) in September and October 2017, respectively. The fruits were authenticated in the Department of Pharmacognosy, Faculty of Pharmacy, *Grigore T. Popa* University of Medicine and Pharmacy (Iasi, Romania). Voucher specimens of *C. mas* (CM4176/2017), *S. aucuparia* (SA4177/2017) and *V. opulus* (VO4178/2017) fruits were deposited in the same department. The fresh fruits were frozen and stored at −20 °C until use.

The frozen fruits (200 g of each) were electrically grinded and subjected to ultrasound-assisted extraction (40 kHz, 3 × 30 min) with 3 × 600 mL of acetone:water:acetic acid mixture (80:19.5:0.5) (v/v/v), similarly to extraction procedures reported in literature (Boeing et al., 2014; Kallio et al., 2014). The extracts from each plant material were combined, filtered and concentrated at 40 °C to 50 mL of aqueous phase. The aqueous phases were delipidated with diethyl ether (10 × 50 mL) by liquid-liquid partition and then lyophilized to yield *C. mas* (CM, yield: 9.65%), *S. aucuparia* (SA, yield: 8.1%) and *V. opulus* (VO, yield: 11.5%) extracts. All extracts were stored at −20 °C until use.

2.3. HPLC-DAD-ESI-Q-TOF-MS/MS analysis

Qualitative high-performance liquid chromatography with diode array detection and electrospray ionization quadrupole time-of-flight tandem mass spectrometry (HPLC-DAD-ESI-Q-TOF-MS/MS) was performed according to a reported method (Luca et al., 2019) with slight modifications. The binary mobile phase consisted of 0.1% formic acid in water (A) and 0.1% formic acid in acetonitrile (B). The following gradient was applied: 0% B (0 min), 40% B (30 min) and 100% B (35 min). The gas temperature was 300 °C. The capillary voltage was set at 4200 V. ESI-Q-TOF-MS spectra were recorded in the mass range of 100–1700 *m/z*.

2.4. Quantitative HPLC-DAD analysis

HPLC-DAD analysis was carried out on a Shimadzu HPLC system as previously described (Luca et al., 2019) with minor changes. The mobile phase consisted of 0.1% formic acid in water (A) and acetonitrile (B). The elution profile was: 10–20% B (0–10 min), 20% B (10–20 min), 20–50% B (20–30 min), 50–100% B (30–33 min) and 100% B (33–45 min). The detection wavelength was set at 254 nm. The concentration of chlorogenic acid was determined from the peak area, using the linear regression equation of the calibration curve obtained from six concentrations of the standard. The results were expressed as mg/g extract.

2.5. Arginase inhibition assay

Arginase inhibition was evaluated by a spectrophotometric assay based on the reaction of urea (product of arginase-catalyzed hydrolysis of L-arginine) and α-isonitrosopropiophenone with the generation of a pink imine monitored at 550 nm (Corraliza et al., 1994; Bordage et al., 2017). For the preliminary screening, each extract was tested at final concentrations of 10 and 100 μg/mL. The percentages of arginase

inhibition were calculated by the conversion of the resulting absorbance [relative to the absorbance of the control (100% arginase activity)]. When inhibition percentages exceeded 70% at 100 μg/mL, concentration giving half-maximal inhibition (IC_{50}) was calculated. Thus, a stock solution (21 mg/mL) of each extract was extemporaneously and successively diluted in water to obtain a series of final concentrations (3000, 900, 300, 90, 30, 9, 3, 0.9 and 0.3 μg/mL). The IC_{50} value was estimated from the nonlinear sigmoidal curve-fitting using Prism® (GraphPad software, version 5.03) after plotting the inhibition percentages *versus* the logarithm of concentration. All the experiments were performed in triplicate.

2.6. Vascular reactivity studies

2.6.1. Animals

Ten male Sprague Dawley rats (8-9 weeks-old) were purchased from Janvier (Le Genest Saint Isle, France). Animals were kept under 12:12 h light-dark cycle at 22 ± 1 °C having free access to standard food and water. The protocol was approved by the local ethics committee for animal experiments no. 2015/001-CD/5 PR of Franche-Comté University (Besançon, France). The investigation complied with the ARRIVE animal research: reporting *in vivo* experiments.

2.6.2. Aortic arteries preparations

The rats were anesthetized with sodium pentobarbital 60 mg/kg (Ceva Santé Animale, France). The aortic rings were obtained from the descending thoracic aorta. The isometric contractile response was recorded by a force transducer associated with IOX2 software as previously described (Bagnost et al., 2008). A passive tension was gradually applied from 0.5 to 2 g during 1 h equilibration period. Then, the aortic rings viability was assessed through vasoconstriction with a high-KCl (100 mM) Krebs solution. Endothelial integrity was confirmed by more than 80% relaxation induced by the endothelium-dependent agonist Ach (10^{-6} M) in the aortic rings preconstricted with PE (10^{-6} M). In some rings, the endothelium was mechanically removed. The completeness of endothelial denudation was confirmed by less than 10% relaxation response to Ach.

2.6.3. Experimental protocols for vascular reactivity

Endothelium-intact and -denuded aortic rings were contracted with PE (10^{-6} M). After reaching the plateau of maximum vasoconstriction, the extracts were cumulatively added in the organ bath (10^{-8}-10^{-2} g/mL). The relaxant effect was calculated as the percent relaxation to the maximal contraction induced by PE. The concentration of extract producing 50% of the maximal relaxation (EC_{50}), maximal relaxation percentage (E_{max}) and area under the curve (AUC) were determined from the cumulative dose-response curves using Prism® (GraphPad software, version 5.03). To evaluate the contribution of eNOS in the vasorelaxant activity of the extracts, the endothelium-intact aortic rings were pre-incubated with L-NAME (eNOS inhibitor, 10^{-4} M) for 30 min before PE (10^{-6} M) induced contraction followed by cumulative addition of CM, SA or VO extract in the organ bath.

2.7. Brine shrimp lethality assay

Artemia franciscana (brine shrimp) was used to assess the toxicity of fruit extracts (Cock and Kalt, 2010; Cock and Van Vuuren, 2015). The test was performed in 24-well plates using different concentrations of each extract (5000, 2500, 1250, 625 and 312 μg/mL). In brief, the nauplii (10–20 nauplii/well) were placed in contact with the test solutions (1.5 mL/well) for 48 h to reach the second or third instar stage of development. All nauplii, dead and alive, were counted at 24 h (Libralato et al., 2016). Artificial seawater was employed as a negative control. The assay was performed in triplicate. The concentration-response curve was non-linearly modelled using the four-parameter logistic model with a robust method based on the sum of squares loss and using the Hessian matrix in the Hill bounds, as implemented in the R package dr4pl (Landis et al., 2019; Ritz et al., 2015); the graphs were generated using the drc R package of R 3.6.0 software. The concentration producing 50% mortality of brine shrimp nauplii (LC_{50}) was calculated using the non-linear regression.

2.8. Statistical analysis

The results were expressed as mean ± SEM. Data were analyzed with Prism® (GraphPad Software, version 5.03). Statistical analysis between percentages of arginase inhibition of different extracts was based on one-way analysis of variance (ANOVA) followed by Bonferroni's test. For vascular reactivity studies, concentration-response curves of each extract in the presence or not of a specific inhibitor were compared by two-way ANOVA for repeated measures. Differences between two values were evaluated by Student's *t*-test or Mann-Whitney test when data were not normally distributed. Values of $p < 0.05$ were considered statistically significant.

3. Results

3.1. Metabolite profiling of fruit extracts

3.1.1. Metabolite profiling of Cornus mas fruit extract

The HPLC-DAD-ESI-Q-TOF-MS/MS analysis of CM extract allowed the annotation of 16 constituents belonging to various phytochemical classes (Fig. 1A, Table 1). Ten organic and phenolic acid derivatives were identified; of these, quinic (**CM1**), tartaric (**CM2**), malic (**CM3**), citric (**CM4**) and chlorogenic (**CM10**) acids were confirmed by comparing their chromatographic and spectral data with those of reference standards. Compounds **CM5**, **CM6** and **CM13** were characterized as glycosides of gallic, hydroxybenzoic and vanillic acids, respectively. The losses of 90 Da ($C_3H_6O_3$) and 120 Da ($C_4H_8O_4$) from the deprotonated ion $[M-H]^-$ at *m/z* 361.0788 (**CM5**) indicated the presence of a sugar unit; furthermore, the fragment ion at *m/z* 169.0149 (corresponding to the deprotonated gallic acid) resulted after the loss of a heptosyl group from the precursor ion. Thus, compound **CM5** was tentatively assigned as gallic acid heptoside (Xue et al., 2014). Similarly, the MS/MS fragment ions generated by compounds **CM6** ($[M-H]^-$ at *m/z* 299.0762) and **CM13** ($[M-H]^-$ at *m/z* 329.0870) allowed their tentative identification as hexosides of hydroxybenzoic and vanillic acids, respectively. Compound **CM7** (*m/z* 337.0925) showed two diagnostic fragment ions at *m/z* 163.0613 (yielded after the loss of quinic acid unit) and 119.0310 (which could result from the decarboxylation of the previous ion). Thus, this compound was tentatively identified as coumaroylquinic acid (Luca et al., 2019). The MS/MS spectrum of the precursor ion at *m/z* 311.0405 (**CM12**) exhibited three main fragment ions at *m/z* 179.0372 [caffeic acid-H]$^-$, 149.0102 [tartaric acid-H]$^-$ and 135.0468 [caffeic acid–CO_2–H]$^-$ that led to putative identification of compound **CM12** as caftaric acid (Chen et al., 2012).

Four iridoid derivatives were spotted in CM extract. Compound **CM8** ($[M-H]^-$ at *m/z* 375.1301) was tentatively identified as loganic acid based on its MS/MS fragmentation pattern which yielded fragment ions at *m/z* 213.0787 [M-glucosyl-H]$^-$, 169.0895 [aglycon–CO_2–H]$^-$ and 151.0801 [aglycon–CO_2–H]$^-$; these data overlapped those suggested by Xue et al. (2014). The mass spectrum of compound **CM9** indicated the presence of an additional group of 116 Da ($C_4H_4O_4$) which could originate from malic acid; this side chain might be attached to loganic acid (suggested by the fragment ion at *m/z* 375.1330). On the other hand, compound **CM11** showed a formic acid adduct $[M + HCOO]^-$ at *m/z* 403.1231; its MS/MS spectrum showed fragment ions at *m/z* 357.1165 $[M-H]^-$, 195.0603 [M-glucosyl-H]$^-$ and 179.0578 [glucose-H]$^-$ that are in agreement with the structure of sweroside, as proposed by Deng et al. (2013). In case of compound **CM15**, the deprotonated ion $[M-H]^-$ at *m/z* 541.1552 suggested the molecular formula $C_{24}H_{30}O_{14}$. The loss of sugar unit afforded the fragment ion at *m/z*

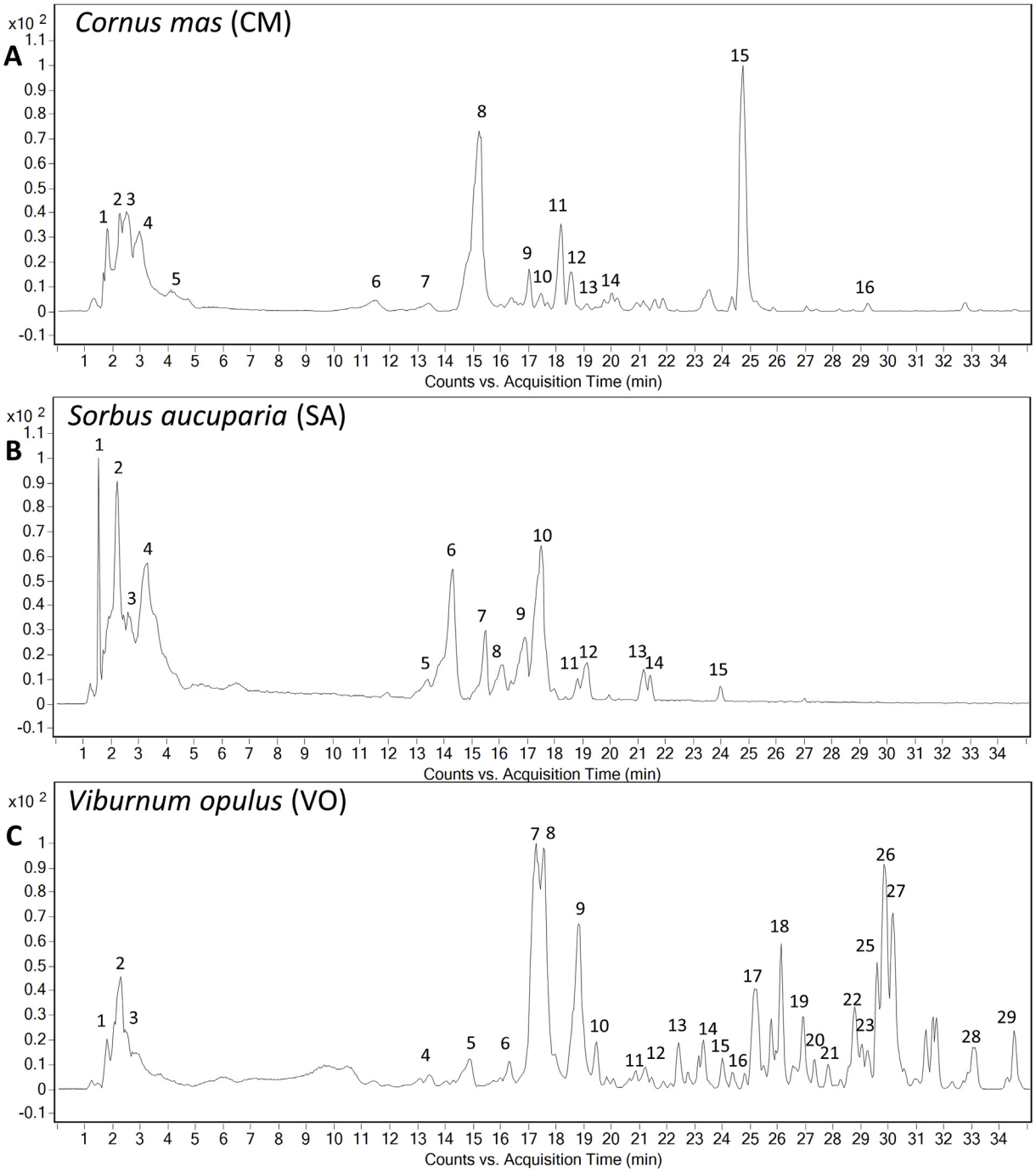

Fig. 1. Base peak chromatograms of *Cornus mas*, *Sorbus aucuparia* and *Viburnum opulus* fruit extracts.

379.1030 which was further cleaved at the esterification site into two fragment ions at *m/z* 209.0858 and 169.0142 (Fig. 2). This led to the assumption that compound **CM15** might belong to cornuside I. Additionally, two flavonoid glycosides were noticed in CM extract. Quercetin (**CM16**) was easily identified by comparing its chromatographic and spectral parameters with those of a commercially available standard. On the other side, aromadendrin hexoside (**CM14**) exhibited a deprotonated ion $[M\text{-}H]^-$ at *m/z* 449.1080 that indicated the molecular formula $C_{21}H_{22}O_{11}$. The loss of the sugar part (162 Da) afforded the fragment ion at *m/z* 287.0490 possibly corresponding to the deprotonated aglycon (aromadendrin) ion (Pawlowska et al., 2010). Further dehydration and decarbonylation led to the fragment ions at *m/z* 269.0388 $[aglycon\text{–}H_2O\text{–}H]^-$ and 259.0580 $[aglycon\text{–}CO\text{–}H]^-$, respectively.

3.1.2. Metabolite profiling of Sorbus aucuparia fruit extract

A number of 15 phytochemical constituents were observed in SA extract (Fig. 1B, Table 2), as follows: sorbitol (**SA1**), two flavonoid glycosides and 12 organic and phenolic acids. The identity of malic (**SA2**), citric (**SA3**), neochlorogenic (**SA6**) and chlorogenic (**SA10**) acids was confirmed by reference substances. As suggested by other authors (Willems et al., 2016), it is possible to differentiate neochlorogenic, chlorogenic and cryptochlorogenic acids on the basis of their major fragment ions. Neochlorogenic acid (**SA6**) generated a major base peak at *m/z* 191.0647 and a relatively abundant peak at *m/z* 179.0459; chlorogenic acid (**SA10**) yielded only one major fragment ion peak at

Table 1
Chromatographic and spectrometric data of the compounds tentatively identified in *Cornus mas* fruit extract.

No	R_T (min)	[M-H]$^-$, *m/z* (δ, ppm)	MF	MS/MS fragment ions (*m/z*)	Tentative assignment	References
CM1	1.8	191.0566 (2.5)	$C_7H_{12}O_6$	173.0451, 127.0409, 111.0475	Quinic acid[a]	Karar and Kuhnert (2015)
CM2	2.3	149.0098 (4.2)	$C_4H_6O_6$	130.9971, 103.0059	Tartaric acid[a]	Deng et al. (2013)
CM3	2.4	133.0145 (1.9)	$C_4H_6O_5$	115.0061	Malic acid[a]	Deng et al. (2013)
CM4	3.0	191.0203 (2.9)	$C_6H_8O_7$	173.0138, 155.0063, 129.0184, 111.0115	Citric acid[a]	Deng et al. (2013)
CM5	4.1	361.0788 (3.2)	$C_{14}H_{18}O_{11}$	271.0495, 211.0253, 169.0142	Gallic acid heptoside	Xue et al. (2014)
CM6	11.5	299.0762 (3.5)	$C_{13}H_{16}O_8$	239.0484, 209.0316, 179.0224, 137.0202	Hydroxybenzoic acid hexoside	Karar and Kuhnert (2015)
CM7	13.4	337.0925 (1.5)	$C_{16}H_{18}O_8$	163.0613, 119.0310	Coumaroylquinic acid	Karar and Kuhnert (2015)
CM8	15.2	375.1301 (3.6)	$C_{16}H_{24}O_{10}$	213.0787, 169.0895, 151.0801	Loganic acid	Xue et al. (2014)
CM9	17.0	491.1417 (2.2)	$C_{20}H_{28}O_{14}$	375.1330, 213.0771, 169.085 151.0695	Loganic acid malyl ester	–
CM10	17.5	353.0883 (1.4)	$C_{16}H_{18}O_9$	191.0376, 179.0131, 173.0207, 161.0059, 135.0266	Chlorogenic acid[a]	Deng et al. (2013)
CM11	18.2	403.1231 (4.1)[b]	$C_{16}H_{22}O_9$	357.1165, 237.0769, 195.0603, 179.0578, 125.0239	Sweroside	Xue et al. (2014)
CM12	18.6	311.0405 (1.1)	$C_{13}H_{12}O_9$	179.0372, 149.0102, 135.0468	Caftaric acid	Chen et al. (2012)
CM13	19.1	329.0870 (2.4)	$C_{14}H_{18}O_9$	209.0438, 167.0324, 123.0436	Vanillic acid hexoside	Karar and Kuhnert (2015)
CM14	20.0	449.1080 (2.1)	$C_{21}H_{22}O_{11}$	287.0490, 269.0388, 259.0580, 151.0033	Aromadendrin hexoside	Pawlowska et al. (2010)
CM15	24.7	541.1552 (1.9)	$C_{24}H_{30}O_{14}$	379.1030, 347.0892, 209.0858, 169.0142, 125.0278	Cornuside I	Xue et al. (2014)
CM16	29.2	301.0354 (0.1)	$C_{15}H_{10}O_7$	151.0045, 131.0028	Quercetin[a]	Karar and Kuhnert (2015)

MF molecular formula.
MS mass spectrum.
R_T retention time.
δ mass error.
[a] Confirmed by standard.
[b] Detected as formic acid adduct.

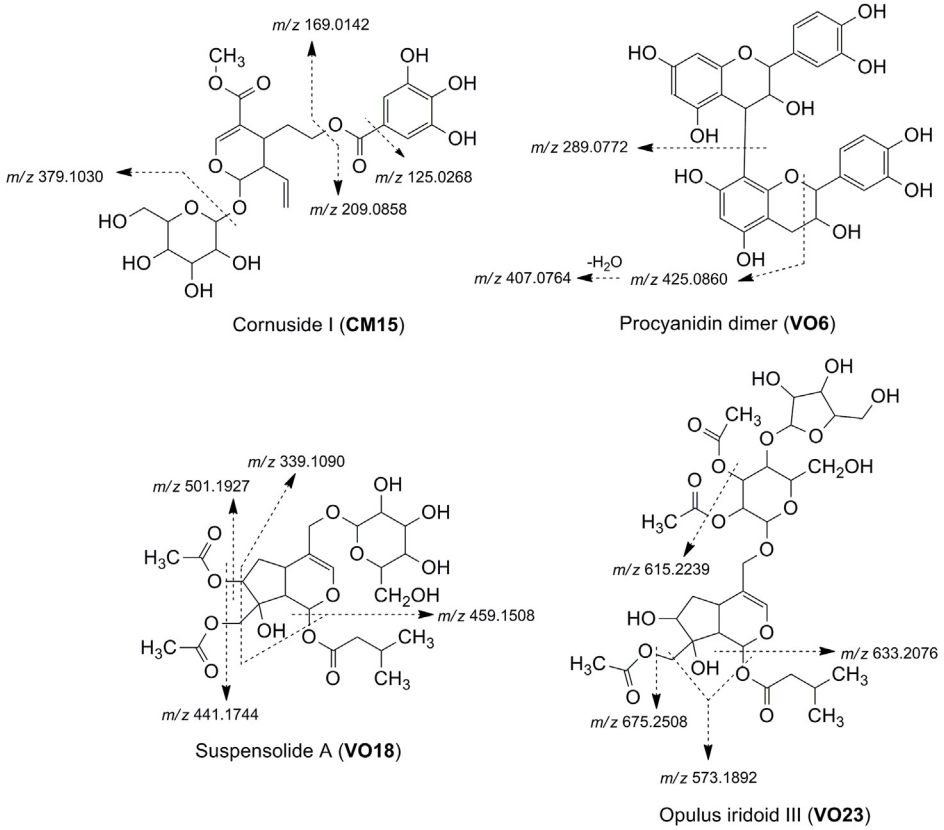

Fig. 2. Proposed structures for the compounds CM15, VO6, VO18 and VO23 tentatively identified by HPLC-DAD-ESI-Q-TOF-MS/MS.

m/z 191.0584, whereas cryptochlorogenic acid (**SA11**) was easily distinguished by a characteristic fragment ion at *m/z* 173.0447. Hydroxybenzoic (**SA4**) and coumaroylquinic (**SA5**) acids as well as benzoic and vanillic acid hexosides (**SA8**, **SA9**, **SA12**) were tentatively identified as described in section 3.1.1. Compound **SA7** ([M-H]$^-$ at *m/z* 367.1038) exhibited the fragment ions at *m/z* 191.0514 [quinic acid-H]$^-$ and 175.0423 [ferulic acid–H_2O–H]$^-$ which led to the tentative assignment of **SA7** as feruloylquinic acid (Mikulic-Petkovsek et al., 2017). As compared to chlorogenic acid, compound **SA13** showed a deprotonated ion [M-H]$^-$ at *m/z* 335.0761 which suggested the molecular formula $C_{16}H_{18}O_8$. In the MS/MS spectrum, the fragment ions corresponding to caffeic acid (*m/z* 179.0370 [caffeic acid-H]$^-$, 161.0293 [caffeic acid–H_2O–H]$^-$ and 135.0491 [caffeic acid–CO_2–H]$^-$) supported the tentative identification of compound **SA13** as caffeoylshikimic acid (Matczak et al., 2018). Additionally, two flavonoid glycosides were spotted in SA extract, namely quercetin dihexoside (**SA14**) and quercetin hexoside (**SA15**). These compounds were tentatively identified based on their pseudomolecular ions at *m/z* 625.1389 and

Table 2
Chromatographic and spectrometric data of the compounds tentatively identified in *Sorbus aucuparia* fruit extract.

No	R_T (min)	[M-H]$^-$, *m/z* (δ, ppm)	MF	MS/MS fragment ions (*m/z*)	Tentative assignment	References
SA1	1.5	181.0716 (0.9)	$C_6H_{14}O_6$	163.0621, 101.0295	Sorbitol	Zymone et al. (2018)
SA2	2.2	133.0145 (1.9)	$C_4H_6O_5$	115.0060	Malic acid[a]	Zymone et al. (2018)
SA3	2.6	191.0206 (4.5)	$C_6H_8O_7$	154.9982, 129.0196, 111.0117	Citric acid[a]	Mikulic-Petkovsek et al. (2017)
SA4	3.3	137.0243 (0.8)	$C_7H_6O_3$	–	Hydroxybenzoic acid	Matczak et al. (2018)
SA5	13.4	337.0930 (0.3)	$C_{16}H_{18}O_8$	163.0508, 119.0341	Coumaroylquinic acid	Mikulic-Petkovsek et al. (2017)
SA6	14.3	353.0886 (2.2)	$C_{16}H_{18}O_9$	191.0647, 179.0459, 161.0457, 135.0500	Neochlorogenic acid[a]	Mikulic-Petkovsek et al. (2017)
SA7	15.5	367.1038 (0.9)	$C_{17}H_{20}O_9$	191.0514, 175.0423	Feruloylquinic acid	Mikulic-Petkovsek et al. (2017)
SA8	16.2	329.0864 (1.7)[b]	$C_{13}H_{16}O_7$	283.0827, 207.0506, 181.0712, 121.0297	Benzoic acid hexoside	Karar and Kuhnert (2015)
SA9	16.9	329.0886 (2.4)	$C_{14}H_{18}O_9$	167.0362, 123.0464	Vanillic acid hexoside 1	Karar and Kuhnert (2015)
SA10	17.5	353.0883 (1.4)	$C_{16}H_{18}O_9$	191.0584, 161.0261	Chlorogenic acid[a]	Mikulic-Petkovsek et al. (2017)
SA11	18.8	353.0875 (0.9)	$C_{16}H_{18}O_9$	191.0520, 173.0447, 161.0266	Cryptochlorogenic acid	Mikulic-Petkovsek et al. (2017)
SA12	19.2	329.0887 (2.7)	$C_{14}H_{18}O_9$	167.0344, 123.0422	Vanillic acid hexoside 2	Karar and Kuhnert (2015)
SA13	21.2	335.0761 (3.4)	$C_{16}H_{18}O_8$	179.0370, 161.0293, 135.0491	Caffeoylshikimic acid	Matczak et al. (2018)
SA14	21.5	625.1389 (3.4)	$C_{27}H_{30}O_{17}$	463.0889, 301.0322, 151.0032	Quercetin dihexoside	Mikulic-Petkovsek et al. (2017)
SA15	24.0	463.0872 (2.1)	$C_{21}H_{20}O_{12}$	301.0307, 151.0050	Quercetin hexoside	Matczak et al. (2018)

MF molecular formula.
MS mass spectrum.
R_T retention time.
δ mass error.
[a] Confirmed by standard.
[b] Detected as formic acid adduct.

463.0872, respectively, and the fragment ion at *m/z* 301.0322 characteristic to quercetin (aglycon).

3.1.3. Metabolite profiling of Viburnum opulus fruit extract

As compared to CM and SA extracts, the HPLC-DAD-ESI-Q-TOF-MS/MS analysis of VO extract revealed a more complex profile (Fig. 1C, Table 3), with 29 constituents (organic and phenolic acids, flavonols,

Table 3
Chromatographic and spectrometric data of the compounds tentatively identified in *Viburnum opulus* fruit extract.

No	R_T (min)	[M-H]$^-$, *m/z* (δ, ppm)	MF	MS/MS fragment ions (*m/z*)	Tentative assignment	References
VO1	1.8	191.0568 (3.8)	$C_7H_{12}O_6$	173.0111, 111.0460	Quinic acid[a]	Karar and Kuhnert (2015)
VO2	2.3	133.0149 (4.9)	$C_4H_6O_5$	114.9997	Malic acid[a]	Deng et al. (2013)
VO3	2.6	191.0220 (4.5)	$C_6H_8O_7$	173.0032, 128.9901, 111.0107	Citric acid[a]	Deng et al. (2013)
VO4	13.4	337.0918 (3.2)	$C_{16}H_{18}O_8$	163.0517, 119.0322	Coumaroylquinic acid	Karacelik et al. (2015)
VO5	15.0	329.0885 (2.1)	$C_{14}H_{18}O_9$	239.0546, 209.0435, 167.0264	Vanillic acid hexoside	Karar and Kuhnert (2015)
VO6	16.3	577.1331 (3.5)	$C_{30}H_{25}O_{12}$	451.0606, 425.0860, 407.0764, 289.0701, 245.0774	Procyanidin dimer	Karacelik et al. (2015)
VO7	17.2	289.0708 (3.3)	$C_{15}H_{14}O_6$	245.0972, 205.0433, 179.0383, 151.0430	Catechin[a]	Karacelik et al. (2015)
VO8	17.5	353.0869 (2.5)	$C_{16}H_{18}O_9$	191.0517, 161.0226	Chlorogenic acid[a]	Kraujalyte et al. (2013)
VO9	18.8	353.0882 (1.1)	$C_{16}H_{18}O_9$	191.0529, 179.0259, 161.0141	Cryptochlorogenic acid	Kraujalyte et al. (2013)
VO10	19.5	289.0710 (2.6)	$C_{15}H_{14}O_6$	245.0872, 205.0479, 179.0398	Epicatechin[a]	Kraujalyte et al. (2013)
VO11	20.9	739.1897 (2.3)	$C_{36}H_{36}O_{17}$	577.1447, 569.1224, 451.0810, 339.0546, 289.0772, 245.0802, 205.0802	Procyanidin dimer hexoside	Karacelik et al. (2015)
VO12	21.2	865.1977 (1.0)	$C_{45}H_{38}O_{18}$	713.1622, 695.1460, 577.1273, 289.0712	Procyanidin trimer	Karacelik et al. (2015)
VO13	22.4	595.1314 (1.5)	$C_{26}H_{28}O_{16}$	463.0865, 301.0298, 151.0129	Quercetin pentoside hexoside	Karacelik et al. (2015)
VO14	23.3	609.1469 (1.3)	$C_{27}H_{30}O_{16}$	463.0464, 301.0371, 271.0166, 255.0171, 150.9936	Rutin[a]	Karacelik et al. (2015)
VO15	24.0	463.0885 (0.6)	$C_{21}H_{20}O_{12}$	301.0348, 271.0291, 151.0056	Quercetin hexoside	Karacelik et al. (2015)
VO16	24.4	447.0940 (1.6)	$C_{21}H_{20}O_{11}$	301.0356, 151.0030	Quercetin rhamnoside	Karacelik et al. (2015)
VO17	25.2	451.1240 (1.3)	$C_{21}H_{24}O_{11}$	341.0732, 289.0713, 245.0418	(Epi)catechin hexoside 1	Di Lecce et al. (2014)
VO18	26.1	607.2232 (2.1)[b]	$C_{25}H_{38}O_{14}$	561.2450, 501.1927, 459.1524, 441.1744,	Suspensolide A	Hase and Iwagawa (1982); Tomassini et al. (1995)
VO19	26.9			417.1528, 339.1090, 231.0811	Viburtinoside IV	
VO20	27.3				Viburtinoside V	
VO21	27.8	451.1245 (0.2)	$C_{21}H_{24}O_{11}$	341.0608, 289.0793, 245.0422	(Epi)catechin hexoside 2	Di Lecce et al. (2014)
VO22	29.2	301.0356 (0.7)	$C_{15}H_{10}O_7$	151.0064, 131.0029	Quercetin[a]	Yurkiv and Grytsyk (2017)
VO23	28.8	781.2802 (3.9)[b]	$C_{32}H_{48}O_{19}$	735.2757, 675.2508, 633.2076, 573.1892,	Opulus iridoid III isomers	Bock et al. (1978)
VO24	29.0			615.2239, 513.1670, 453.1359		
VO25	29.6	649.2328 (3.5)[b]	$C_{27}H_{40}O_{15}$	603.2204, 543.2081, 501.1614, 483.1806,	Opulus iridoid II isomers	Bock et al. (1978)
VO26	29.8			381.1170		
VO27	30.2					
VO28	33.0	691.2454 (0.1)[b]	$C_{29}H_{42}O_{16}$	645.2401, 561.1774, 501.1612	Tetraacetyl (iso)suspensolide F	Tomassini et al. (1997)
VO29	34.6					

MF molecular formula.
MS mass spectrum.
R_T retention time.
δ mass error.
[a] Confirmed by standard.
[b] Detected as formic acid adduct.

Table 4
Arginase inhibitory activity of *Cornus mas*, *Sorbus aucuparia* and *Viburnum opulus* fruit extracts.

Extract/ positive control	Arginase inhibition (%) at 10 μg/mL[a]	Arginase inhibition (%) at 100 μg/mL[a]	IC_{50} (μg/mL)
CM	15.79 ± 0.90[b]	36.90 ± 1.80[a]	n.d.
SA	12.2 ± 1.98[b]	27.70 ± 1.72[a]	n.d.
VO	29.81 ± 1.47[a]	67.95 ± 1.00[c]	71.02 ± 3.06
nor-NOHA	91.4 ± 0.77	99.9 ± 0.34	0.3134 ± 0.012

Values represent mean of percentage inhibition ± SEM of three different experiments performed in triplicate. Values with a statistical significance ($p < 0.05$) are annotated with different letters; n.d. = not detected; CM = *Cornus mas*; SA = *Sorbus aucuparia*; VO = *Viburnum opulus;* nor-NOHA = Nω-hydroxy-nor-arginine.

[a] The reference arginase inhibitor (nor-NOHA) was tested in concentrations of 10 and 100 μM.

flavanols and iridoid glycosides) being fully or partially identified. Quinic (**VO1**), malic (**VO2**), citric (**VO3**), coumaroylquinic (**VO8**), chlorogenic and cryptochlorogenic (**VO9**) acids, as well as vanillic acid hexoside (**VO5**) were annotated as described in sections 3.1.1 and 3.1.2. Quercetin (**VO22**) and four of its glycosides, quercetin pentoside hexoside (**VO13**), rutin (**VO14**), quercetin hexoside (**VO15**) and quercetin rhamnoside (**VO16**), were identified based on their characteristic pseudomolecular and fragment ions, especially the diagnostic ion at *m/z* 301.0356 corresponding to the deprotonated aglycon (Karacelik et al., 2015). The identities of compounds **VO7** ($[M-H]^-$ at *m/z* 289.0708) and **VO10** ($[M-H]^-$ at *m/z* 289.0710) were established by comparison with reference catechin and epicatechin, respectively. Moreover, two (epi) catechin hexosides (**VO17** and **VO21**) were also tentatively characterized on the basis of their $[M-H]^-$ ions at *m/z* 451.1240 and 451.1245, respectively with MS/MS spectra indicating the (epi)catechin nature of the aglycon unit (Di Lecce et al., 2014). Compound **VO6** was tentatively ascribed to a procyanidin dimer on the basis of its deprotonated $[M-H]^-$ ion at *m/z* 577.1331 and diagnostic fragment ions. As suggested by Verardo et al. (2008), the Retro-Diels-Alder fission of the flavonoid skeleton (loss of $C_8H_8O_3$) could explain the fragment ion at *m/z* 425.0860 which, after water elimination, generated the fragment at *m/z* 407.0764. The cleavage of the interflavan carbon-carbon bond produced the ion at *m/z* 289.0701 corresponding to the monomeric unit, whilst the further loss of 44 Da (C_2H_4O) in the benzofuran skeleton yielded the ion at *m/z* 245.0774 (Fig. 2). Compound **VO11** ($[M-H]^-$ at *m/z* 739.1897) showed an additional hexose unit (162 Da). As the fragment ions were similar to those of the procyanidin dimer **VO6** (*m/z* 577.1447, 451.0810, 289.0772, 245.0802), compound **VO11** was tentatively labeled as procyanidin dimer hexoside (Karacelik et al., 2015). In case of compound **VO12**, the deprotonated ion $[M-H]^-$ at *m/z* 865.1977, as well as its MS/MS fragment ions at *m/z* 713.1622 $[M–C_8H_8O_3–H]^-$, 577.1273 $[dimer-H]^-$ and 289.0712 $[monomer-H]^-$, indicated a procyanidin trimer type structure (Verardo et al., 2008).

Finally, several iridoid glycosides were annotated in VO extract. Since their distribution is limited only to some *Viburnum* species, there were not enough MS literature data and, thus, their assignment should be treated as purely tentative. Compounds **VO18, VO19, VO20** are isomers with molecular formula $C_{25}H_{38}O_{14}$. The fragment ions at *m/z* 501.1927 $[M-acetic\ acid-H]^-$, 459.1524 $[M-(iso)valeric\ acid-H]^-$, 441.1744 $[M-2 \times acetic\ acid-H]^-$, 417.1528 $[M-acetic\ acid-(iso)valeryl-H]^-$ and 339.1090 $[M-2 \times acetic\ acid-(iso)valeric\ acid-H]^-$, observed in their MS/MS spectra, pointed out the sequential neutral losses of two acetic acid and one (iso)valeric acid groups (Fig. 2). Suspensolide A, viburtinosides IV and V, three iridoid glycosides previously reported in *V. suspensum* and *V. tinus* (Hase and Iwagawa, 1982; Tomassini et al., 1995), have the same molecular formula and mass spectral behavior.

The deprotonated $[M-H]^-$ ions of compounds **VO23** and **VO24** suggested the same molecular formula $C_{32}H_{48}O_{19}$; the fragment ions at *m/z* 675.2508 $[M-acetic\ acid-H]^-$, 633.2076 $[M-(iso)valeric\ acid-H]^-$, 615.2239 $[M-2 \times acetic\ acid-H]^-$, 573.1892 $[M-acetic\ acid-(iso)valeryl-H]^-$, 513.1770 $[M-2 \times acetic\ acid-(iso)valeric\ acid-H]^-$ and 453.1359 $[M-3 \times acetic\ acid-(iso)valeric\ acid-H]^-$ indicated this time the presence of three acetic acid and one (iso)valeric acid groups (Fig. 2). There is one known iridoid glycoside isolated from *V. opulus* that might exhibit this MS/MS spectral pattern, namely opulus iridoid III (Bock et al., 1978). Opulus iridoid III has the same aglycon as suspensolide A and viburtinosides IV and V, but it contains three acetyl, one (iso)valeryl and one xylosyl units attached to its aglycon skeleton. As compared to compounds **VO23** and **VO24**, the molecular formula of isomers **VO25-VO27** ($C_{27}H_{40}O_{15}$) suggested the lack of the second sugar (pentose) unit. Consequently, the following fragment ions were noticed at *m/z* 543.2081 $[M-acetic\ acid-H]^-$, 501.1614 $[M-(iso)valeric\ acid-H]^-$, 483.1806 $[M-2 \times acetic\ acid-H]^-$ and 381.1180 $[M-3 \times acetic\ acid-(iso)valeric\ acid-H]^-$. One known structure that might possibly fulfill these spectral requirements is represented by opulus iridoid II (Bock et al., 1978). Finally, compounds **VO28** and **VO29**, with the same suggested molecular formula $C_{29}H_{42}O_{16}$, afforded MS/MS fragment ions at *m/z* 561.1774 $[M-(iso)valeryl-H]^-$ and 501.1612 $[M-acetic\ acid-(iso)valeryl-H]^-$. There are three known isomers with the same molecular formula and MS fragmentation pattern, already reported in *V. ayavacense*: 7,10,2″,3″-tetra-*O*-acetylisosuspensolide F, 7,10,2″,6″-tetra-*O*-acetylisosuspensolide F and 7,10,2″,3″-tetra-*O*-acetylsuspensolide F (Tomassini et al., 1997). Structurally, they differ not only in the positions of the four acetyl groups but also in the type of the pentanoyl group (isovaleryl in suspensolide F derivative and 2-methylbutanoyl in isosuspensolide F derivatives).

3.2. Chlorogenic acid levels in fruit extracts

VO extract contained significantly ($p < 0.05$) higher levels of chlorogenic acid (30.89 ± 0.40 mg/g) as compared to CM and SA extracts (0.72 ± 0.01 and 2.03 ± 0.01 mg/g, respectively).

3.3. Arginase inhibitory activity of fruit extracts

CM, SA and VO extracts were screened for their ability to inhibit bovine arginase I. As shown in Table 4, at 100 μg/mL, CM and SA extracts induced less than 50% inhibition whereas VO extract produced more than 60% inhibition of arginase activity. Thus, VO extract was further investigated for concentration-response arginase inhibition and an IC_{50} value of 71.02 ± 3.06 μg/mL was determined (Table 4).

3.4. Vasorelaxant effects of fruit extracts

All extracts produced a dose-dependent vasorelaxation in the endothelium-intact aortic rings reaching E_{max} values higher than 96% (Fig. 3A–C, Table 5). Notably, VO extract exhibited the most remarkable activity characterized by the lowest EC_{50} value (6.3 ± 1.6 μg/mL) as compared to SA and CM extracts (EC_{50} values of 78.5 ± 8.6 and 100.9 ± 11.6 μg/mL, respectively). Endothelium removal significantly abolished the vasorelaxant effects of all extracts indicating a strong endothelium-dependent vasorelaxation (Fig. 3A–C). As shown in Fig. 3A–C, L-NAME, an eNOS inhibitor, suppressed the vasorelaxant effects of all extracts; the suppression of vasorelaxation was also confirmed by a decrease of area under the curve (AUC) values (Table 5).

3.5. Brine shrimp toxicity of fruit extracts

Brine shrimp toxicity test was used to evaluate the acute toxicity (expressed as LC_{50} values) of the fruit extracts towards *Artemia franciscana*. LC_{50} values higher than 1000 μg/mL indicate lack of toxicity, LC_{50} values ranging from 500 to 1000 μg/mL predict a weak toxicity and LC_{50} values lower than 500 μg/mL indicate toxicity (Déciga-

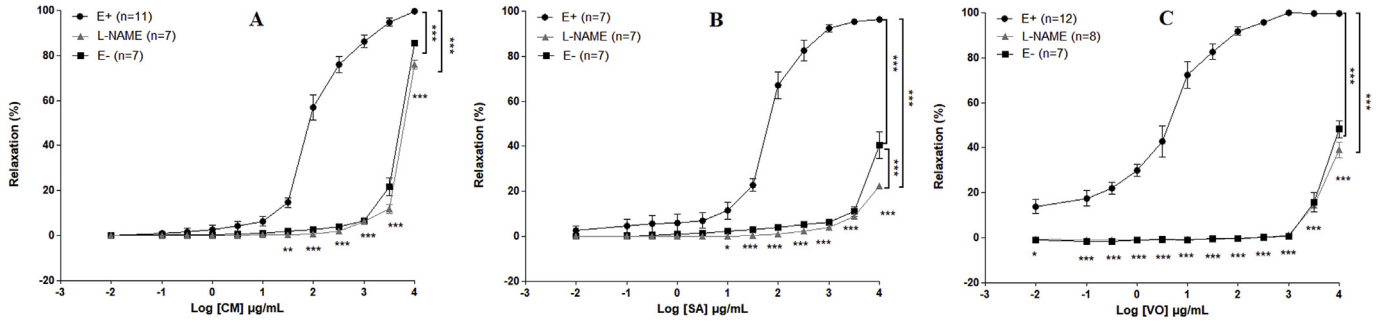

Fig. 3. Cumulative concentration-vasorelaxant response curves for *Cornus mas* (A), *Sorbus aucuparia* (B) and *Viburnum opulus* (C) fruit extracts in the endothelium-intact (E+) and endothelium-denuded (E−) aortic rings precontracted with PE (10^{-6} M). Effects of L-NAME (10^{-4} M) on each fruit extract-induced vasorelaxation were evaluated.

Values represent mean ± SEM of *n* individual aortic rings from different animals. *p < 0.05, **p < 0.01, ***p < 0.001 *versus* endothelium-intact (E+) induced vasorelaxation; CM = *Cornus mas*; SA = *Sorbus aucuparia*; VO = *Viburnum opulus*; PE = phenylephrine; L-NAME = N(ω)-nitro-L-arginine-methyl-ester.

Table 5

EC_{50}, E_{max} and AUC values of *Cornus mas*, *Sorbus aucuparia* and *Viburnum opulus* fruit extracts-induced relaxation in the endothelium-intact (E+) and endothelium-denuded (E−) aortic rings in the absence or presence of L-NAME.

Extract	EC_{50} (µg/mL)	E_{max} (%)	AUC	n
Endothelium-intact (E+)				
CM	100.9 ± 11.63	99.82 ± 0.88	197.6 ± 7.98	11
SA	78.52 ± 8.59	96.30 ± 0.52	224.2 ± 13.04	7
VO	6.31 ± 1.61	100.3 ± 2.22	297.2 ± 18.21	12
+L-NAME				
CM	–	76.11 ± 1.98*	29.88 ± 1.72*	7
SA	–	22.27 ± 1.23*	13.65 ± 1.28*	7
VO	–	39.00 ± 3.48*	15.13 ± 3.33*	8
Endothelium-denuded (E−)				
CM	–	85.61 ± 1.04*	41.09 ± 3.95*	7
SA	–	40.39 ± 5.97*	27.32 ± 4.71*	7
VO	–	48.22 ± 3.70*	11.16 ± 3.07*	7

Values are means ± SEM of *n* individual aortic rings from different rats. E_{max} is the maximal relaxation in the PE-induced contraction. AUC is the area under the curve; CM = *Cornus mas*; SA = *Sorbus aucuparia*; VO = *Viburnum opulus*; PE = phenylephrine; L-NAME = N(ω)-nitro-L-arginine-methyl-ester. *p < 0.0001 when comparing *versus* E_{max} or AUC of the endothelium-intact (E+) rings.

Campos et al., 2007; Meyer et al., 1982). Thus, all three extracts proved to be non-toxic on *Artemia franciscana* nauplii as shown by the relatively high LC_{50} values and 95% confidence interval (CI) (LC_{50} = 1100 µg/mL with 95% CI = 1033–1171 for CM extract, LC_{50} = 2271 µg/mL with 95% CI = 2208–2335 for SA extract, LC_{50} = 3610 µg/mL with 95% CI = 3481–3744 for VO extract).

4. Discussion

The present study provides the first evidence of the endothelium-dependent vasorelaxant effects of *C. mas, S. aucuparia* and *V. opulus* fruit extracts together with a comprehensive metabolite profiling of fruit extracts.

The extracts were obtained from frozen fruits. In contrast to the ambient air-drying or oven-drying methods, freezing maintains the stability of phytochemicals to a greater extent (Lohachoompol et al., 2004; Sultana et al., 2012). In addition, as freezing is one of the most commonly used methods for preserving fruits, the present study aimed to determine if the consumption of frozen fruits might have cardiovascular benefits.

With regard to CM extract, our study indicated the presence of not only organic and phenolic acid derivatives, but also iridoids such as loganic acid, sweroside, aromadendrin hexoside and cornuside I. Our data are in agreement with a previous study on a methanolic extract of *C. mas* fruits that reported ten constituents among which five organic and phenolic acids (citric, tartaric, malic, gallic and chlorogenic acids), four iridoids (loganic acid, loganin, sweroside, cornuside) and one flavonoid (rutin). In the ethanolic fraction of an aqueous fruit extract, 24 constituents were identified, notably 7-*O*-galloyl-D-sedoheptulose, 1,7-di-*O*-galloyl-D-sedoheptulose, loganic acid, loganin, cornuside, sweroside, morroniside and caffeic acid (Xue et al., 2014). Furthermore, Pawlowska et al. (2010) reported eight flavonoid glycosides in a methanolic fruit extract, namely 3-*O*-xyloside, rhamnoside, rutinoside, galactoside and glucoside of quercetin, aromadendrin-7-*O*-glucoside and kaempferol-3-*O*-galactoside.

Our study on SA extract identified predominantly organic and phenolic acids. The phytochemical profile of SA extract is consistent with previous literature data that reported the presence of two phenolic acids (chlorogenic and neochlorogenic acids) and eight mono- and di-glycosides of quercetin and kaempferol in the fruit juice (Gil-Izquierdo and Mellenthin, 2001; Mikulic-Petkovsek et al., 2017). Furthermore, neochlorogenic and chlorogenic acids, rutin, hyperoside and quercetin were also reported in the 50% ethanolic fruit extract (Savikin et al., 2017).

In contrast to previous extracts, VO extract showed a diverse phytochemical profile that included organic and phenolic acids, flavonols, flavanols and iridoids. Previous reports already described a similar phenolic profile (phenolic acids, flavonols, flavanols) in the fruit juices (Kraujalyte et al., 2013; Karacelik et al., 2015). On the basis of HPLC-DAD data, Velioglu et al. (2006) reported not only chlorogenic acid, catechin, epicatechin, but also cyanidin-3-rutinoside, cyanidin-3-glucoside and various different glycosides of quercetin (xyloside, rutinoside, glucoside, arabinoside, rhamnoside) in the fruit juice. The present study provided the new finding that *V. opulus* fruits contain several iridoid glycosides. *Viburnum* genus is known to accumulate this category of compounds, but mainly in leaves or branches (Tomassini et al., 1997; Gao et al., 2018). However, even if their annotation is purely tentative and their structures were not fully elucidated due to the limitations of the MS technique, there are plenty of clues indicating the presence of this category of compounds in the relatively more non-polar part of the base peak chromatogram of VO extract (more than 35% acetonitrile in the mobile phase). One possible explanation for the inconsistencies with literature data might be the fact that 80% acetone acidified with 0.5% acetic acid was used as extraction solvent, while in the previous studies the fruit juice was directly processed and analyzed. Juice extraction is mainly based on the diffusion of water-soluble constituents, whereas organic solvents (acidified acetone-water mixtures) might increase the extractability of relatively non-polar compounds, such as iridoids. For instance, the methanolic or hydroethanolic extracts of other fruits (*C. mas*) were shown to contain iridoid glycosides, such as loganic acid, loganin, sweroroside or cornuside (Xue et al., 2014).

From a quantitative point of view, the present study showed that VO extract had a higher content in chlorogenic acid in comparison with CM and SA extracts. Other studies also reported that *V. opulus* fruits represent a dietary source of chlorogenic acid (2.037 mg/kg fresh berries) (Velioglu et al., 2006). Variable amounts of chlorogenic acid were also found in *C. mas* fruits (32.76 and 135 mg/100 g fresh weight) (Moldovan et al., 2016; Sochor et al., 2014) and *S. aucuparia* fruits (1.22 mg/g dry weight) (Gaivelyte et al., 2013). Among the polyphenolic compounds known to inhibit arginase, chlorogenic acid is considered to be one of the most efficient inhibitors (IC_{50} = 3.73 μg/mL) (Bordage et al., 2017). Thus, it is tempting to connect the chlorogenic acid content of VO extract with its potent arginase inhibitory effect. Other compounds present in VO extract, even less efficient than chlorogenic acid, such as epicatechin, quercetin, caffeic acid, might also contribute to its arginase inhibitory activity (Bordage et al., 2017). The arginase inhibitory activity of VO extract is comparable to other extracts tested using the same protocol such as the methanolic extract of *Rhus tripartita* stems (IC_{50} = 71.48 μg/mL) or the dichloromethane extract of *Retama raetam* stems (IC_{50} = 84.91 μg/mL) (Attia et al., 2019).

It is well known that arginase competes with eNOS for the common substrate, L-arginine (Caldwell et al., 2015). Thus, the extract with the highest arginase inhibitory effect is expected to have the strongest capacity to enhance eNOS activity and, as a consequence, to vasodilate isolated vessels. Moreover, the arginase inhibitory activity of VO extract might increase NO bioavailability inside the endothelial cells thus preventing endothelial dysfunction. Our study supports this assumption as, among the three extracts, VO extract showed the most potent arginase inhibitory and vasodilating effects. The three extracts induced endothelium-dependent and eNOS-dependent vasorelaxant effects, which is consistent with the available data on the positive effects of polyphenolic compounds on endothelial function (Schini-Kerth et al., 2010). This is also compatible with previous studies reporting that chlorogenic acid induced an endothelium-dependent vasorelaxation by activating NO in aortic rings (Tom et al., 2016) and protected against hypochlorite-induced endothelial dysfunction (Jiang et al., 2016). The vasorelaxant effects of tested extracts are comparable to other plant extracts investigated in rat aortic rings precontracted with PE (10^{-6} M) such as the methanolic extracts of *Carex cuprina* roots (EC_{50} = 4.3 μg/mL) and *Cyperus eragostis* seeds (EC_{50} = 3.9 μg/mL) or the water decoction of *Harungana madagascariensis* stem barks (EC_{50} = 80 μg/mL) (Arraki et al., 2017; Lemba Tom et al., 2018). Further studies are necessary to determine if this *ex vivo* positive activity on the endothelial function might be translated into an antihypertensive effect and/or a reduction in the endothelial dysfunction *in vivo*.

All three extracts proved to be non-toxic towards *Artemia franciscana* in acute exposure. According to the LC_{50} values, VO extract was less toxic than SA and CM extracts. Literature reports reasonably good correlations between the brine shrimp lethality and the acute oral toxicity in mice (Logarto et al., 2001). More specifically, Logarto et al. (2001) showed that LC_{50} values over 25 μg/mL in brine shrimps translate into acute oral median lethal doses (LD_{50}) of 2500–8000 mg/kg. According to Hodge and Sterner toxicity scale, the aforementioned LD_{50} values indicate slight toxicity (500–5000 mg/kg) or lack of toxicity (5000–15,000 mg/kg) (Ahmed, 2015). Our data are in agreement with *in vivo* studies of acute toxicity reporting *C. mas* fruits to be safe for consumption in rats (up to 5 g/kg) and humans (100 g of fresh fruits/day) (Dinda et al., 2016). No previous data exist on the toxicity of *S. aucuparia* and *V. opulus* fruits, but both fruits are reported to be edible (Konarska and Domaciuk, 2018; Mrkonjić et al., 2017). However, further animal studies are needed to evaluate the toxicity of VO, SA and CM extracts in acute and long-term ingestion.

5. Conclusions

In summary, our findings provided the first evidence that *Cornus mas*, *Sorbus aucuparia* and *Viburnum opulus* fruit extracts exhibit endothelium-dependent vasorelaxant properties relying on eNOS activation and arginase inhibition, without acute toxic effects in brine shrimps. These positive vascular effects could be, at least in part, attributed to the presence of chlorogenic acid. Among the three extracts tested, *Viburnum opulus* fruit extract appears as the most promising for the treatment of diseases associated with endothelial dysfunction.

Conflicts of interest

The authors declare no conflict of interest.

Declaration of interests

The authors declare that they have no known competing financial interests or personal relationships that could have appeared to influence the work reported in this paper.

Acknowledgements

A.B. would like to acknowledge UEFISCDI (The Romanian Executive Unit for Higher Education, Research, Development and Innovation Funding) for the financial support provided through mobility projects for researchers PN-III-P1-1.1-MC-2017-0452 and PN-III-P1-1.1-MC-2018-1848.

Appendix A. Supplementary data

Supplementary data to this article can be found online at https://doi.org/10.1016/j.fct.2019.110764.

References

Ahmed, M., 2015. Acute toxicity (lethal dose 50 calculation) of herbal drug somina in rats and mice. Pharmacol. Pharm. 6, 185–189.
Almeida Rezende, B., Pereira, A.C., Cortes, S.F., Lemos, V.S., 2016. Vascular effects of flavonoids. Curr. Med. Chem. 23, 87–102.
Arraki, K., Totoson, P., Decendit, A., Badoc, A., Zedet, A., Jolibois, J., Pudlo, M., Demougeot, C., Girard-Thernier, C., 2017. Cyperaceae species are potential sources of natural mammalian arginase inhibitors with positive effects on vascular function. J. Nat. Prod. 80, 2432–2438.
Asgary, S., Rafieian-Kopaei, M., Adelnia, A., Kazemi, S., Shamsi, F., 2010. Comparing the effects of lovastatin and *Cornus mas* fruit on fibrinogen level in hypercholesterolemic rabbits. ARYA Atheroscler. 6, 1–5.
Attia, R., Messaoud, C., Arraki, K., Zedet, A., Demougeot, C., Boussaïd, M., Girard, C., 2019. Phytochemical screening and arginase inhibitory activity of extracts from several Tunisian medicinal plants. South Afr. J. Bot. 120, 313–318.
Bagnost, T., Berthelot, A., Bouhaddi, M., Laurant, P., Andre, C., Guillaume, Y., 2008. Treatment with the arginase inhibitor N(omega)-hydroxy-nor-L-arginine improves vascular function and lowers blood pressure in adult spontaneously hypertensive rat. J. Hypertens. 26, 1110–1118.
Bock, K., Jensen, S.R., Nielsen, B.J., Norn, V., 1978. Iridoid allosides from *Viburnum opulus*. Phytochemistry 17, 753–757.
Boeing, J.S., Barizão, E.O., E Silva, B.C., Montanher, P.F., de Cinque Almeida, V., Visentainer, J.V., 2014. Evaluation of solvent effect on the extraction of phenolic compounds and antioxidant capacities from the berries: application of principal component analysis. Chem. Cent. J. 8, 48.
Bordage, S., Pham, T.N., Zedet, A., Guglielmetti, A.S., Nappey, M., Demougeot, C., Girard-Thernier, C., 2017. Investigation of mammal arginase inhibitory properties of natural ubiquitous polyphenols by using an optimized colorimetric microplate assay. Planta Med. 83, 647–653.
Caldwell, R.B., Toque, H.A., Narayanan, S.P., Caldwell, R.W., 2015. Arginase: an old enzyme with new tricks. Trends Pharmacol. Sci. 36, 395–405.
Česoniene, L., Daubaras, R., Viškelis, P., Šarkinas, A., 2012. Determination of the total phenolic and anthocyanin contents and antimicrobial activity of *Viburnum opulus* fruit juice. Plant Foods Hum. Nutr. 67, 256–261.
Chen, H.J., Inbaraj, B.S., Chen, B.H., 2012. Determination of phenolic acids and flavonoids in *Taraxacum formosanum* Kitam by liquid chromatography-tandem mass spectrometry coupled with a post-column derivatization technique. Int. J. Mol. Sci. 13, 260–285.
Cock, I.E., Kalt, F.R., 2010. Toxicity evaluation of *Xanthorrhoea johnsonii* leaf methanolic extract using the *Artemia franciscana* bioassay. Pharmacogn. Mag. 6, 166–171.
Cock, I.E., Van Vuuren, S.F., 2015. A comparison of the antimicrobial activity and toxicity of six *Combretum* and two *Terminalia* species from southern Africa. Pharmacogn. Mag. 11, 208–218.
Corraliza, I.M., Campo, M.L., Soler, G., Modolell, M., 1994. Determination of arginase activity in macrophages: a micromethod. J. Immunol. Methods 174, 231–235.

Déciga-Campos, M., Rivero-Cruz, I., Arriaga-Alba, M., Castañeda-Corral, G., Angeles-López, G.E., Navarrete, A., Mata, R., 2007. Acute toxicity and mutagenic activity of Mexican plants used in traditional medicine. J. Ethnopharmacol. 110, 334–342.

Deng, S., West, B.J., Jensen, C.J., 2013. UPLC-TOF-MS characterization and identification of bioactive iridoids in *Cornus mas* fruit. J. Anal. Methods Chem. 7. Article ID 710972. https://doi.org/10.1155/2013/710972.

Di Lecce, G., Arranz, S., Jauregui, O., Tresserra-Rimbau, A., Quifer-Rada, P., Lamuela-Raventos, R.M., 2014. Phenolic profiling of the skin, pulp and seeds of Albariño grapes using hybrid quadrupole time-of-flight and triple-quadrupole mass spectrometry. Food Chem. 145, 874–882.

Dinda, B., Kyriakopoulos, A.M., Dinda, S., Zoumpourlis, V., Thomaidis, N.S., Velegraki, A., Markopoulos, C., Dinda, M., 2016. *Cornus mas* L. (cornelian cherry), an important European and Asian traditional food and medicine: ethnomedicine, phytochemistry and pharmacology for its commercial utilization in drug industry. J. Ethnopharmacol. 193, 670–690.

Durante, W., 2013. Role of arginase in vessel wall remodeling. Front. Immunol. 4, 111.

Gaivelyte, K., Jakstas, V., Razukas, A., Janulis, V., 2013. Variation in the contents of neochlorogenic acid, chlorogenic acid and three quercetin glycosides in leaves and fruits of Rowan (*Sorbus*) species and varieties from collections in Lithuania. Nat. Prod. Commun. 8, 1105–1110.

Gao, Y., Yang, W.Q., Yang, K., Jiang, X.J., Li, X.M., Wang, F., 2018. New iridoid glycosides from *Viburnum punctatum*. Phytochem. Lett. 28, 145–148.

Gil-Izquierdo, A., Mellenthin, A., 2001. Identification and quantitation of flavonols in rowanberry (*Sorbus aucuparia* L.) juice. Eur. Food Res. Technol. 213, 12–17.

Girard-Thernier, C., Pham, T.N., Demougeot, C., 2015. The promise of plant-derived substances as inhibitors of arginase. Mini Rev. Med. Chem. 15, 798–808.

Hasse, T., Iwagawa, T., 1982. Bitter principles of *Viburnum suspensum*. Chem. Lett. 11, 13–14.

Hurlimann, D., Ruschitzka, F., Lüscher, T.F., 2002. The relationship between the endothelium and the vessel wall. Eur. Heart J. 4 (Suppl. A), A1–A7. https://doi.org/10.1016/S1520-765X(02)90067-2.

Jiang, R., Hodgson, J.M., Mas, E., Croft, K.D., Ward, N.C., 2016. Chlorogenic acid improves *ex vivo* vessel function and protects endothelial cells against HOCl-induced oxidative damage, via increased production of nitric oxide and induction of Hmox-1. J. Nutr. Biochem. 27, 53–60.

Kallio, H., Yang, W., Liu, P., Yang, B., 2014. Proanthocyanidins in wild sea buckthorn (*Hippophaë rhamnoides*) berries analyzed by reversed-phase, normal-phase, and hydrophilic interaction liquid chromatography with UV and MS detection. J. Agric. Food Chem. 62, 7721–7729.

Karacelik, A.A., Kucuk, M., Iskefiyeli, Z., Aydemir, S., Smet, S.D., Miserez, B., Sandra, P., 2015. Antioxidant components of *Viburnum opulus* L. determined by on-line HPLC–UV–ABTS radical scavenging and LC–UV–ESI-MS methods. Food Chem. 175, 106–114.

Karar, M.G.E., Kuhnert, N., 2015. UPLC-ESI-Q-TOF-MS/MS characterization of phenolics from *Crataegus monogyna* and *Crataegus laevigata* (hawthorn) leaves, fruits and their herbal derived drops (Crataegutt Tropfen). J. Chem. Biol. Ther. 1, 102. https://doi.org/10.4172/2572-0406.1000102.

Konarska, A., Domaciuk, M., 2018. Differences in the fruit structure and the location and content of bioactive substances in *Viburnum opulus* and *Viburnum lantana* fruits. Protoplasma 255, 25–41.

Kraujalyte, V., Venskutonis, P.R., Pukalskas, A., Cesoniene, L., Daubaras, R., 2013. Antioxidant properties and polyphenolic compositions of fruits from different European cranberrybush (*Viburnum opulus* L.) genotypes. Food Chem. 141, 3695–3702.

Kucharska, A.Z., Szumny, A., Sokół-Łętowska, A., Piórecki, N., Klymenko, S.V., 2015. Iridoids and anthocyanins in cornelian cherry (*Cornus mas* L.) cultivars. J. Food Compos. Anal. 40, 95–102.

Landis, J.T., An, H., Bailey, A.G., Dittmer, D.P., Marron, J.S., 2019. dr4pl: Dose Response Data Analysis Using the 4 Parameter Logistic (4pl) Model. https://CRAN.R-project.org/package=dr4pl, Accessed date: 21 January 2019.

Le Brocq, M., Leslie, S.J., Milliken, P., Megson, I.L., 2008. Endothelial dysfunction: from molecular mechanisms to measurement, clinical implications, and therapeutic opportunities. Antioxidants Redox Signal. 10, 1631–1674.

Lemba Tom, E.N., Mimb, J.R.B., Nyunaï, N., Bekono, Y.F., Longo, F., Fogue, S.K., Dimo, T., 2018. Vasodilatory effects of aqueous extract from *Harungana madagascariensis* stem bark in isolated rat aorta: the roles of endothelium and K+ channels. Am. J. Ethnomed. 5, 1–8.

Lerman, A., Zeiher, A.M., 2005. Endothelial function: cardiac events. Circulation 111, 363–368.

Libralato, G., Prato, E., Migliore, L., Cicero, A.M., Manfra, L., 2016. A review of toxicity testing protocols and endpoints with *Artemia* spp. Ecol. Indicat. 69, 35–49.

Lohachoompol, V., Srzednicki, G., Craske, J., 2004. The change of total anthocyanins in blueberries and their antioxidant effect after drying and freezing. J. Biomed. Biotechnol. 5, 248–252.

Logarto, P.A., Silva, Y.R., Guerra, S.I., Iglesias, B.L., 2001. Comparative study of the assay of *Artemia salina* L. and the estimate of the medium lethal dose (LD50 value) in mice, to determine oral acute toxicity of plant extracts. Phytomedicine 8, 395–400.

Luca, S.V., Miron, A., Aprotosoaie, A.C., Mihai, C.T., Vochita, G., Gherghel, D., Ciocarlan, N., Skalicka-Wozniak, K., 2019. HPLC-DAD-ESI-Q-TOF-MS/MS profiling of *Verbascum ovalifolium* Donn ex Sims and evaluation of its antioxidant and cytogenotoxic activities. Phytochem. Anal. 30, 34–45.

Lucas, R., Fulton, D., Caldwell, R.W., Romero, M.J., 2014. Arginase in the vascular endothelium: friend or foe? Front. Immunol. 5, 589.

Manjolin, L.C., dos Reis, M.B., Maquiaveli, Cdo C., Santos-Filho, O.A., da Silva, E.R., 2013. Dietary flavonoids fisetin, luteolin and their derived compounds inhibit arginase, a central enzyme in *Leishmania amazonensis* infection. Food Chem. 141, 2253–2262.

Matczak, M., Marchelak, A., Michel, P., Owczarek, A., Piszczan, A., Kolodziejczyk-Czepas, J., Nowak, P., Olszewska, M.A., 2018. *Sorbus domestica* L. leaf extracts as functional products: phytochemical profiling, cellular safety, pro-inflammatory enzymes inhibition and protective effects against oxidative stress *in vitro*. J. Funct. Foods 40, 207–218.

Meyer, B., Ferrigni, N., Putnam, J., Jacobsen, L., Nichols, D., McLaughlin, J., 1982. Brine shrimp: a convenient general bioassay for active plant constituents. Planta Med. 45, 31–34.

Mikulic-Petkovsek, M., Krska, B., Kiprovski, B., Veberic, R., 2017. Bioactive components and antioxidant capacity of fruits from nine *Sorbus* genotypes. J. Food Sci. 82, 647–658.

Minozzo, B., Fernandes, D., Beltrame, F., 2018. Phenolic compounds as arginase inhibitors: new insights regarding endothelial dysfunction treatment. Planta Med. 84, 277–295.

Moldovan, B., Filip, A., Clichici, S., Suharoschi, R., Bolfa, P.F., David, L., 2016. Antioxidant activity of Cornelian cherry (*Cornus mas* L.) fruits extract and the in vivo evaluation of its anti-inflammatory effects. J. Funct. Foods 26, 77–87.

Mrkonjić, Z., Nađpal, J., Beara, I., Sabo, V.A., Četojević-Simin, D., Mimica-Dukić, N., 2017. Phenolic profiling and bioactivities of fresh fruits and jam of *Sorbus* species. J. Serb. Chem. Soc. 82, 651–664.

Olszewska, M.A., Michel, P., 2009. Antioxidant activity of inflorescences, leaves and fruits of three *Sorbus* species in relation to their polyphenolic composition. Nat. Prod. Res. 23, 1507–1521.

Pawlowska, A.M., Camangi, F., Braca, A., 2010. Quali-quantitative analysis of flavonoids of *Cornus mas* L. (Cornaceae) fruits. Food Chem. 119, 1257–1261.

Prati, C., Berthelot, A., Kantelip, B., Wendling, D., Demougeot, C., 2012. Treatment with the arginase inhibitor Nw-hydroxy-nor-L-arginine restores endothelial function in rat adjuvant-induced arthritis. Arthritis Res. Ther. 14, R130. https://doi.org/10.1186/ar3860.

Ritz, C., Baty, F., Streibig, J.C., Gerhard, D., 2015. Dose-response analysis using R. PLoS One 10, e0146021. https://doi.org/10.1371/journal.pone.0146021.

Savikin, K.P., Zdunic, G.M., Krstic-Milosevic, D.B., Sircelj, H.J., Stesevici, D.D., Pljevljakusic, D.S., 2017. *Sorbus aucuparia* and *Sorbus aria* as a source of antioxidant phenolics, tocopherols, and pigments. Chem. Biodivers. 14. https://doi.org/10.1002/cbdv.201700329.

Schini-Kerth, V.B., Auger, C., Kim, J.H., Etienne-Selloum, N., Chataigneau, T., 2010. Nutritional improvement of the endothelial control of vascular tone by polyphenols: role of NO and EDHF. Pflug. Arch. Eur. J. Phy. 459, 853–862.

Sochor, J., Jurikova, T., Ercisli, S., Mlcek, J., Baron, M., Balla, S., Ylmaz, S.O., Necas, T., 2014. Characterization of cornelian cherry (*Cornus mas* L.) genotypes–genetic resources for food production in Czech Republic. Genetika 46, 915–924.

Sultana, B., Anwar, F., Ashraf, M., Saari, N., 2012. Effect of drying techniques on the total phenolic contents and antioxidant activity of selected fruits. J. Med. Plants Res. 6, 161–167.

Timmis, A., Townsend, N., Gale, C., Grobbee, R., Maniadakis, N., Flather, M., 2018. European society of cardiology: cardiovascular disease statistics 2017. Eur. Heart J. 39, 508–579.

Tom, E.N.L., Girard-Thernier, C., Demougeot, C., 2016. The Janus face of chlorogenic acid on vascular reactivity: a study on rat isolated vessels. Phytomedicine 23, 1037–1042.

Tomassini, L., Cometa, M.F., Foddai, S., Nicoletti, M., 1995. Iridoid glucosides from *Viburnum tinus*. Phytochemistry 38, 423–425.

Tomassini, L., Foddai, S., Nicoletti, M., Cometa, M.F., Palazzino, G., Galeffi, C., 1997. Iridoid glucosides from *Viburnum ayavacense*. Phytochemistry 46, 901–905.

Velioglu, Y.S., Ekici, L., Poyrazoglu, E.S., 2006. Phenolic composition of European cranberrybush (*Viburnum opulus* L.) berries and astringency removal of its commercial juice. Int. J. Food Sci. Technol. 41, 1011–1015.

Verardo, V., Bonoli, M., Marconi, E., Caboni, M.F., 2008. Determination of free flavan-3-ol content in barley (*Hordeum vulgare* L.) air-classified flours: comparative study of HPLC-DAD/MS and spectrophotometric determinations. J. Agric. Food Chem. 56, 694–698.

Willems, J.L., Khamis, M.M., Saeid, W.M., Purves, R.W., Katselis, G., Low, N.H., El-Aneed, A., 2016. Analysis of a series of chlorogenic acid isomers using differential ion mobility and tandem mass spectrometry. Anal. Chim. Acta 933, 164–174.

Xue, C., Zhang, A., Sun, H., Han, Y., Zou, D., Wang, Y., Wu, X., Wang, W., 2014. An improved ultra-performance liquid chromatography-electrospray ionization/quadrupole-time-of-flight high-definition mass spectrometry method for determining ingredients of herbal *Fructus corni* in blood samples. Pharmacogn. Mag. 10, 422–429.

Yigit, D., 2018. Antimicrobial and antioxidant evaluation of fruit extract from *Cornus mas* L. Aksaray J. Sci. Eng. 2, 41–51.

Yurkiv, K., Grytsyk, A., 2017. HPLC-analysis of phenolic compounds of European cranberry bush fruits (*Viburnum opulus* L.). Pharma Innov. J. 6, 526–529.

Zymone, K., Raudone, L., Raudonis, R., Marska, M., Ivanauskas, L., Janulis, V., 2018. Phytochemical profiling of fruit powder of twenty *Sorbus* L. cultivars. Molecules 23, 2593. https://doi.org/10.3390/molecules23102593.